NASA TECHNICAL NOTE

NASA TN D-5119

c. 1

NASA TN D-5119

ANNEALING OF 22-, 40-, AND 158-MeV PROTON DAMAGE IN n- AND p-TYPE SILICON

by Marvin E. Beatty III and Gerald F. Hill

Langley Research Center
Langley Station, Hampton, Va.

NATIONAL AERONAUTICS AND SPACE ADMINISTRATION • WASHINGTON, D. C. • APRIL 1969

ANNEALING OF 22-, 40-, AND 158-MeV PROTON DAMAGE IN n- AND p-TYPE SILICON

By Marvin E. Beatty III and Gerald F. Hill

Langley Research Center
Langley Station, Hampton, Va.

NATIONAL AERONAUTICS AND SPACE ADMINISTRATION

For sale by the Clearinghouse for Federal Scientific and Technical Information
Springfield, Virginia 22151 – CFSTI price $3.00

ANNEALING OF 22-, 40-, AND 158-MeV PROTON DAMAGE IN n- AND p-TYPE SILICON

By Marvin E. Beatty III and Gerald F. Hill
Langley Research Center

SUMMARY

Studies on n- and p-type silicon irradiated with 22-, 40-, and 158-MeV protons and annealed at 100° C, 200° C, and 300° C are reported. The results show that proton damage is very complex and difficult to anneal in comparison with electron damage. A fluence dependence was found for protons in which the annealing decreased as the fluence increased; this dependence is compared with results previously reported for electrons. It was also found that the annealing increases as the proton energy increases. An unexpected result, alternate increases and decreases in minority-carrier lifetime during isothermal annealing, is discussed.

INTRODUCTION

The annealing processes in silicon will govern the degree of recovery of solar-cell power supplies which are damaged by a space radiation environment. The proton spectrum for a typical orbit (350 nautical miles, 30° inclination) in the Van Allen radiation belt has been calculated by using the trajectory environment codes in reference 1 and is shown in figure 1. Long exposures to this radiation spectrum can result in serious degradation of electronic systems. Studies of annealing of radiation damage in silicon solar-cell power supplies have shown the possibility of using some form of annealing apparatus to improve the output of solar cells damaged by space radiation (ref. 2).

Most of the experimental studies have involved neutron or electron bombardment (refs. 2 to 4). Little work has been reported on the annealing of proton damage in silicon (refs. 5 and 6).

Of the physical properties of semiconductors, one of the more sensitive to ionizing radiation is the minority-carrier lifetime – the average time that excess minority carriers (holes or electrons) will exist before they are reduced to a factor of 1/e of their original number by the recombination process. It was, therefore, chosen as the damage criterion in this experiment. The recovery of lifetime after irradiation of n- and p-type silicon is reported for annealing at 100° C, 200° C, and 300° C. Most of the data are for irradiation with 22-MeV protons; however, a comparison of annealing of 22-, 40-, and 158-MeV proton damage is presented.

The experiments were conducted with commercial silicon solar cells, and the annealing results are reported for the bulk layer where most of the radiation damage and annealing occurs.

SYMBOLS

D_τ	percentage of defects remaining
$\frac{dN}{dE}$	number of particles per unit energy
I	interstitial
V	vacancy
τ	minority-carrier lifetime
τ_o	initial minority-carrier lifetime
τ_x	minority-carrier lifetime after x hours of annealing
ϕ	particle fluence

THEORETICAL BACKGROUND

Proton and electron irradiation of silicon can cause large disorders in the normal lattice structure by displacing silicon atoms from their usual positions, producing vacancies and interstitials. At room temperature, these vacancies and interstitials will quickly recombine and no permanent effect will be noted. Watkins and Corbett (ref. 7), however, have found that in n-type silicon irradiated with low-energy electrons, impurity atoms are trapped to form complex defect centers. The defect centers are not readily annealed at room temperature. In the samples tested for this report, the room-temperature annealing was less than 5 percent.

Watkins and Corbett have found, by spectroscopic analysis, two main impurity defect centers: E-centers and A-centers. The locations of these defect centers and a defect called the divacancy within the silicon lattice are shown in figure 2. The top left lattice illustrates phosphorus-doped (n-type) silicon containing an interstitial oxygen atom. When this particular lattice configuration is bombarded, several types of defects may be formed.

The lattice in the top right of the figure shows an oxygen-vacancy pair which is referred to as the A-center. The E-center, as shown in the lower left of figure 2, is formed when a vacancy pairs with the phosphorus atom. Another type of center is the divacancy, which is simply the coupling of two vacancies. This center is illustrated in the lower right of figure 2.

Figure 3 shows the defect centers in their energy position between the valence and conduction bands for phosphorus-doped (n-type) silicon. It was found (ref. 7) that in n-type silicon manufactured by the float-zone process, which has phosphorus and oxygen impurities of approximately equal concentrations $\left(\text{at least } 10^{15}\ \text{cm}^{-3}\right)$, the E-center dominates. In Czochralski grown (pulled) silicon, the oxygen concentration is much greater $\left(10^{18}\ \text{cm}^{-3}\right)$ than the phosphorus concentration $\left(10^{15}\ \text{cm}^{-3}\right)$ and the A-center dominates. A breakup of these defects and any divacancies that are present are responsible for the major annealing observed in n-type silicon at room temperature and above.

Defect centers have been observed in electron-irradiated p-type silicon; however, an exact model for these centers has not been obtained. It is possible that A-centers exist, as in electron-irradiated n-type silicon, and also a center similar to the E-center. This center would not be neutral as is the E-center, but would have a positive charge due to the impurity atom (boron, aluminum, etc.). There is no experimental evidence to back this supposition, but if it is true, damaged p-type silicon should anneal in a manner similar to damaged n-type silicon.

The defects created when silicon is irradiated with protons are similar to those found with electrons. However, the heavy mass of the proton causes much larger defect centers and possible clustering of defects, and thus results in a more complex damage center. Therefore, proton damage is expected to be less affected by annealing than electron damage.

EXPERIMENTAL TECHNIQUE

Before irradiation, the minority-carrier lifetime was determined for 1.0 ohm-cm silicon samples of both n-type and p-type by an experimental procedure previously employed by the authors (ref. 8). In this method a monochromatic infrared light source is used to generate a current in the base layer of a p-n junction solar cell. This current value is then applied to equations presented in reference 8 to determine minority-carrier lifetime.

Next, the silicon samples were mounted on a target wheel (shown in figs. 4 and 5) with electrical connections to remote test equipment. The samples were irradiated to the desired fluence, the proton beam was stopped, and the desired parameters were measured. The wheel was rotated by remote control, so that a new sample could be placed in target position without the experimenter entering the target room.

Silicon samples of both n-type and p-type (with resistivity of 1.0 ohm-cm and initial minority-carrier lifetime τ_0 of 5.0±0.5 μsec) were irradiated at the Oak Ridge 86-inch cyclotron. Damage by various proton fluences was examined to ascertain the effects of total proton fluence on annealing characteristics. The incident proton energy was determined in each experiment by plotting a standard number-distance curve. Corrections were made for energy losses in beam-pipe windows, ionization-chamber windows, and air. After all of these corrections were considered, the energy of the proton beam was found to be 22 MeV.

The proton fluence incident upon the silicon samples was determined by using an ionization chamber which was calibrated by means of a standard iron-foil activation analysis and a Faraday cup. Energy and flux measurements are estimated to be accurate within ±5 percent and ±10 percent, respectively.

Experiments with n- and p-type silicon were also carried out at the University of Minnesota's 40-MeV linear accelerator, and n-type silicon was tested at the Harvard University's 158-MeV cyclotron. Measurement procedures in these tests were similar to those used with 22-MeV protons.

All the irradiations were performed at room temperature with a flux between 10^7 and 10^9 protons/cm^2-sec. With this flux, heating of the samples is negligible.

After irradiation, the samples were kept in dry ice to prevent room-temperature annealing until temperature studies could be performed. Then the samples were mounted on ceramic plates for the annealing tests. The annealing was done in an oven where the temperature of anneal was controlled to ±5° C. At least three samples of each type of silicon irradiated with 22- and 40-MeV protons were annealed isothermally at 100° C, 200° C, and 300° C for periods up to 12 hours. The n-type silicon samples irradiated with 158-MeV protons were annealed at 100° C and 200° C. Experiments were also conducted with samples which had been irradiated to different fluences to determine the dependence of annealing on different levels of proton irradiation.

After the annealing oven reached the desired temperature, samples were placed inside the oven and left to anneal for some given time period. The samples were then removed from the oven and cooled to room temperature with a high-speed fan. Once the samples reached room temperature, the necessary measurements were made and then they were placed back in the oven for another period of anneal.

The minority-carrier lifetime measurements are used to define the fraction of defects remaining in the silicon. The fraction of defects remaining is found by comparing τ_x, the minority-carrier lifetime after x hours of annealing, with τ_0, the minority carrier lifetime before irradiation. The formula, which represents the unnormalized percentage of damage remaining, is

$$D_\tau = \left(1 - \frac{\tau_x}{\tau_o}\right) \times 100$$

It is used in this report so that the data can be compared with data obtained by many experimenters who have previously used this equation (refs. 2, 5, 6, and 8). This type of curve is useful in that it shows how much radiation damage was induced in the sample prior to annealing as well as the amount of recovery of the sample during increasing annealing time.

Measurements of the minority-carrier lifetime were made at several time intervals during the isothermal annealing tests. In order to examine more closely the rapid increase in τ observed in these measurements, some samples were annealed for 15-minute intervals during the first few hours of testing.

The annealing-oven temperature was monitored by using a copper-constantan thermocouple, and the minority-carrier lifetime was measured at room temperature. Each data point in the figures represents an average of three samples with initial minority-carrier lifetime of 5 ± 0.5 μsec. At any time during each annealing test, the variation in the values of τ for the three samples was less than 3 percent.

EXPERIMENTAL RESULTS

Figure 6 shows the results for p-type silicon samples irradiated with 22-MeV protons to a fluence of 10^{11} protons/cm^2 and annealed at various temperatures for times up to 12 hours. There is a small amount of annealing at 100° C and 200° C (as much as 5 percent at 100° C and 10 percent at 200° C), but annealing at 300° C is much greater (as much as 22 percent). Most of the annealing process seems to occur in less than 2 hours. After 2 hours of annealing, approximately 5 percent of the defects introduced by the protons are annealed at 200° C, while about 18 percent are annealed at 300° C. After 12 hours of annealing, about 10 percent of the defects are annealed at 200° C and 22 percent at 300° C. The general trend of the curves indicates that higher annealing temperatures would probably anneal more of the damage than the 22 percent at 300° C. This would probably be the case until some maximum temperature was reached where damage to the sample caused by thermal effects would offset the annealing of the radiation damage. The annealing oven used for these tests would not go higher than 300° C, and annealing apparatus used on space vehicles probably will not yield temperatures much higher than 300° C.

Figure 7 is a similar plot for n-type silicon. A rapid decrease in the number of defects in the material is followed by a slower, more gradual, decrease. About 10 percent of the defects were annealed at 100° C during a 12-hour period. At 200° C, the fast-annealing portion of the curve indicates a reduction of approximately 20 percent of the defects, and about 25 percent are annealed after 12 hours. At 300° C, about 30 percent of the defects are annealed rapidly and about 40 percent are annealed after 6 hours. Then the curve begins to level off.

Figure 8 shows a closer comparison of the annealing characteristics of n- and p-type silicon at 300° C. This figure points out the fact that although radiation damage is greater in n-type silicon than in p-type, the n-type silicon anneals more than p-type.

Figure 9 depicts the difference in the annealing process in p-type silicon at 200° C for different fluences of 22-MeV protons. The p-type silicon shows very little annealing for $\phi = 5 \times 10^{12}$ protons/cm^2. Annealing is somewhat greater for $\phi = 10^{11}$ protons/cm^2, which is still a relatively high proton fluence compared with that expected for a 1-year mission in space. It was not possible to make measurements for lower proton fluences in these tests, but the trend of the curves indicates that greater annealing efficiency will be achieved as the total fluence is decreased. A similar effect was found for electron fluence by Fang (ref. 2); however, the dependence of annealing on fluence is much stronger for proton damage than for electron damage.

Figure 10 shows a more pronounced fluence dependence in n-type silicon annealed at 300° C. The general trend of the curves indicates the possibility that defects produced by proton fluences less than 10^{11} protons/cm^2, such as those encountered in space, will anneal rapidly at 300° C or above. Very little annealing (less than 10 percent) was noted for a fluence of 5×10^{12} protons/cm^2.

Figure 11 is a comparison of the annealing of 22-, 40-, and 158-MeV proton damage for n-type silicon at 200° C. The annealing trends are similar, with 158-MeV damage being annealed out to a greater degree. These curves and those of figure 10 seem to point out that more complex damage is produced by protons of higher fluence and less energy. It is possible that most of the damage by low fluences of protons with energy greater than 40 MeV can be annealed out at 300° C or above.

The annealing pattern was investigated more thoroughly by making lifetime measurements after successive 15-minute annealing periods. The results of these tests are shown in figure 12 for n- and p-type silicon irradiated to a fluence of 1×10^{12} protons/cm^2. The minority-carrier lifetime τ is plotted against annealing time at 300° C. There is an immediate increase in τ which tapers off after about 1/2 hour of annealing in n-type silicon and 1 hour in p-type, followed by a decrease in τ. After annealing of n-type silicon for about 3 hours and p-type for about 2 hours, τ again begins to increase. Figure 13 shows a similar plot for $\phi = 1 \times 10^{10}$ protons/cm^2. The peak for n-type silicon is not as predominant for this lower fluence. For p-type silicon, the peak is much broader and final recovery does not begin until about $4\frac{1}{2}$ hours, compared with 2 hours in figure 12. In figure 13, recovery was greater than for the higher fluence in figure 12, which is consistent with the fluence dependence of annealing previously discussed.

Figure 14 shows the variation of minority-carrier lifetime with annealing time for p-type silicon irradiated to various fluences of 22-MeV protons and annealed at 300° C. It can be seen that the initial peak in the minority-carrier lifetime occurs earlier and is much sharper as the fluence becomes larger. After this peak occurs, the time required for annealing to increase the minority-carrier lifetime decreases as the fluence increases.

Figure 15 shows the dependence of the recovery of minority-carrier lifetime on proton energy. This plot is representative of silicon samples irradiated with 22- and 40-MeV protons with a total fluence of 10^{12} protons/cm^2 and annealed at 300° C for intervals up to 8 hours. No samples irradiated with 158-MeV protons were tested at 300° C. The general trends of the constructive and destructive annealing processes do not show much energy dependence (at least between 22- and 40-MeV protons). The peak of the annealing curve appears slightly sharper for 22-MeV protons than for 40-MeV protons, but both peaks occur at about the same time. The constructive annealing part of the curve for 40-MeV protons increases much more rapidly than that for 22-MeV protons, which is consistent with the energy-dependence annealing previously discussed.

DISCUSSION OF RESULTS

In experiments to determine the annealing properties of electron-irradiated silicon (mainly n-type), a large amount of defect annealing has been observed (refs. 2 to 4). Even complete recovery of the minority-carrier lifetime has occurred in some cases when the electron fluences were not too high.

The results from the proton experiments and electron experiments are similar in that a rapid annealing is followed by a more gradual annealing; however, the degree of annealing is higher for electron-produced defects (which was expected since protons produce more complex defect centers in the lattice structure).

Hasiguti and Ishino (ref. 9) have summarized general trends of various annealing processes as shown in figure 16, which is for irradiation with 1 to 2 MeV electrons and fluence of 10^{14} to 10^{16} electrons/cm^2. The possible annealing of the interstitial (I) and vacancy (V) are shown to occur mainly below room temperature; therefore, the annealing of these simple defects probably does not affect the annealing reported for protons. The E, A, C, and J centers are possible complex defects, which are shown at the temperatures where various investigators believe they begin to be annealed. According to this figure, the E-center begins to be annealed at about 400° K (125° C) and the A-center at about 500° K (225° C).

Superimposed on the figure are annealing curves for n- and p-type silicon irradiated with 22-MeV protons to $\phi = 10^{11}$ protons/cm^2 and annealed for 12 hours at 300° C (from the experiments reported in this paper). The n- and p-type silicons, although not damaged to the same extent by proton irradiation, seem to be annealing in a similar manner up to 575° K (300° C). In comparison with the electron data, the proton data show much greater magnitude of damage produced and less annealing. At 475° K (200° C), approximately 30 percent of the electron-induced defects remain while 65 percent to 75 percent of the proton-induced defects remain. At 575° K (300° C), a negligible number of electron defects are left, while 45 percent to 60 percent of the proton damage remains.

The annealing curves for electron damage show that n-type silicon and p-type silicon (solid line and dashed line, respectively) anneal at almost the same rate from 475° K (200° C) to 575° K (300° C). The proton-damage curves show n-type annealing to be greater than p-type by about 20 percent, although the n-type silicon was damaged more than the p-type initially. This might indicate that the defects in p-type silicon, while not as numerous, are more complex and harder to anneal. The reverse annealing shown for electron damage was observed by one experimenter; no reverse annealing was seen in proton-damage studies.

The results of the proton annealing experiments depict annealing processes which are similar for n- and p-type silicon. The amount of annealing varies greatly, depending on proton energy, temperature, and total fluence, but the shapes of the annealing curves are very similar. There is a rapid decrease in the number of radiation-induced defects in the silicon, followed by a slower, more gradual decrease.

It is impossible to determine the exact damage mechanisms being annealed in proton-irradiated silicon from these experiments. Some assumptions can be made from the results of Watkins and Corbett (ref. 7). The fast recovery during the first hour or so of annealing at 200° C and 300° C in n-type silicon has been observed in electron-damage annealing, and is attributed to the dissociation of the E-centers. Since the temperature of annealing is in the same range, and the curve slopes are similar for proton and electron annealing, it is probable that the E-center is present in proton-damaged silicon also. The later, more gradual recovery may be the beginning of dissociation of the harder to anneal A-center. The defects which do not anneal are either a large number of A-centers which have not received enough energy to dissociate or more complex defect centers.

The differences between annealing of damage in n- and p-type silicon may be due to defects in p-type silicon that are more complex than the E-center in n-type silicon. The portion of the curve attributed to A-center annealing for n-type silicon had approximately the same slope as the corresponding portion of the curve for p-type silicon. Therefore, it is assumed that p-type silicon may have A-center defects.

The fluence dependence of annealing shown in figures 9 and 10 could be due to that large magnitude of the A-centers being formed at higher fluences. It is possible that the A-centers, as a result of their dense population, are combining to form defect centers even more complex and difficult to anneal.

The dependence of annealing on the energy of the damaging protons, figure 11, is consistent with the energy damage results for protons in silicon (ref. 10). These results indicate that lower energy protons produce more damage than higher energy protons.

The annealing peaks in figure 12 seem to indicate a complex damage mechanism. It appears that competing annealing processes occur during isothermal annealing.

The effects of this constructive and destructive annealing can be important to the electrical performance of a spacecraft whose power systems will depend on annealing of radiation damage. The output of the power system could depend on the time during the annealing process that power is required. It is not known whether these peaks would occur under continuous annealing of power systems subjected to a lower flux.

CONCLUSIONS

A study of isothermal annealing of proton damage in n- and p-type silicon has resulted in the following conclusions:

1. Proton damage is harder to anneal than electron damage.

2. Annealing in both n- and p-type silicon is fluence dependent. Damage from higher proton fluences does not anneal as readily as damage from lower fluences.

3. As the proton energy exceeds 22 MeV, the annealing of the defects becomes greater. This is consistent with energy damage results for protons found by other investigators.

4. Measurements of minority-carrier lifetime taken at short intervals during annealing at 300° C show a rapid increase in lifetime followed by a gradual decrease during the first 2 hours of annealing. After 2 hours, a gradual increase in lifetime is observed. These changes indicate some type of competing annealing processes.

5. For 1.0 ohm-cm silicon, the recovery of the minority-carrier lifetime is slightly greater in n-type than in p-type. This is believed to be the result of a defect center produced by protons in p-type that is more complex than the E-center in n-type.

6. Both types of silicon initially exhibit rapid annealing at 200° C and 300° C which is probably due to a center such as the E-center in n-type and its analog defect center in p-type. The slow annealing of defects after this is believed to be dissociation of A-centers.

7. The results obtained indicate that thermal annealing of silicon solar cells which are heavily damaged by protons will produce some improvement in operation. However, the degree of recovery is not as great as that observed for electron damage.

8. Constructive and destructive annealing processes, which appear as peaks when minority-carrier lifetime is plotted against hours of annealing, are observed in both n- and p-type silicon. The peaks are broader for p-type silicon but become sharper as proton energy and flux are increased. These peaks would lead to fluctuations in current output of the power supplies which could affect a satellite's electronic system. Further studies should be made to determine the exact cause and effect of these fluctuations.

9. Further experiments are needed to determine the response of solar cells that are being irradiated by very low flux (more closely approximating real space flux) and annealed simultaneously.

Langley Research Center,
National Aeronautics and Space Administration,
Langley Station, Hampton, Va., January 17, 1969,
124-09-12-09-23.

REFERENCES

1. Barton, J. A.; Doherty, W. R.; and Hahn, P. G.: A Computer Program Incorporating the Whitaker Threat Model Into the Space Radiation Environment and Shielding Computer Program. WL TR-65-10, U.S. Air Force, May 1965. (Available from DDC as AD 616 106.)

2. Fang, P. H.: Thermal Annealing of Radiation Damage in Solar Cells. X-713-65-468, NASA Goddard Space Flight Center, Nov. 1965.

3. Inuishi, Y.; and Matsuura, K.: Radiation Damage and Annealing of Carrier Life-time in Silicon. J. Phys. Soc. Jap., vol. 18, suppl. III, Mar. 1963, pp. 240-245.

4. Saito, H.; Hirata, M.; and Horiuchi, T.: Annealing of Radiation Defects in Silicon Single Crystals. J. Phys. Soc. Jap., vol. 18, suppl. III, Mar. 1963, pp. 246-250.

5. Faraday, Bruce J.; Statler, Richard L.; and Tauke, Regina V.: Thermal Annealing of Proton-Irradiated Silicon Solar Cells. Conference Record of the Sixth Photovoltaics Specialists Conference, Vol. III, Inst. Elec. Electron. Eng., Mar. 1967, pp. 15-34.

6. Beatty, Marvin E. III; and Hill, Gerald F.: Annealing of High Energy Proton Damage in Silicon. Conference Record of the Sixth Photovoltaics Specialists Conference, Vol. III, Inst. Elec. Electron. Eng., Mar. 1967, pp. 35-52.

7. Watkins, G. D.; and Corbett, J. W.: Defects in Irradiated Silicon. I. Electron Spin Resonance of the Si-A Center. Phys. Rev., Second ser., vol. 121, no. 4, Feb. 15, 1961, pp. 1001-1014.

8. Beatty, Marvin E.; and Hill, Gerald F.: Effect of 40-MeV Protons on Semiconductors as Determined With an Improved Method of Measuring Diffusion Length of Minority Carriers. NASA TN D-2817, 1965.

9. Hasiguti, R. R.; and Ishino, S.: Defect Mobility and Annealing in Irradiated Germanium and Silicon. 7th International Conference on the Physics of Semiconductors. 3 – Radiation Damage in Semiconductors, Academic Press, c.1965, pp. 259-273.

10. Rosenzweig, W.; Smits, F. M.; and Brown, W. L.: Energy Dependence of Proton Irradiation Damage in Silicon. J. Appl. Phys., vol. 35, no. 9, Sept. 1964, pp. 2707-2711.

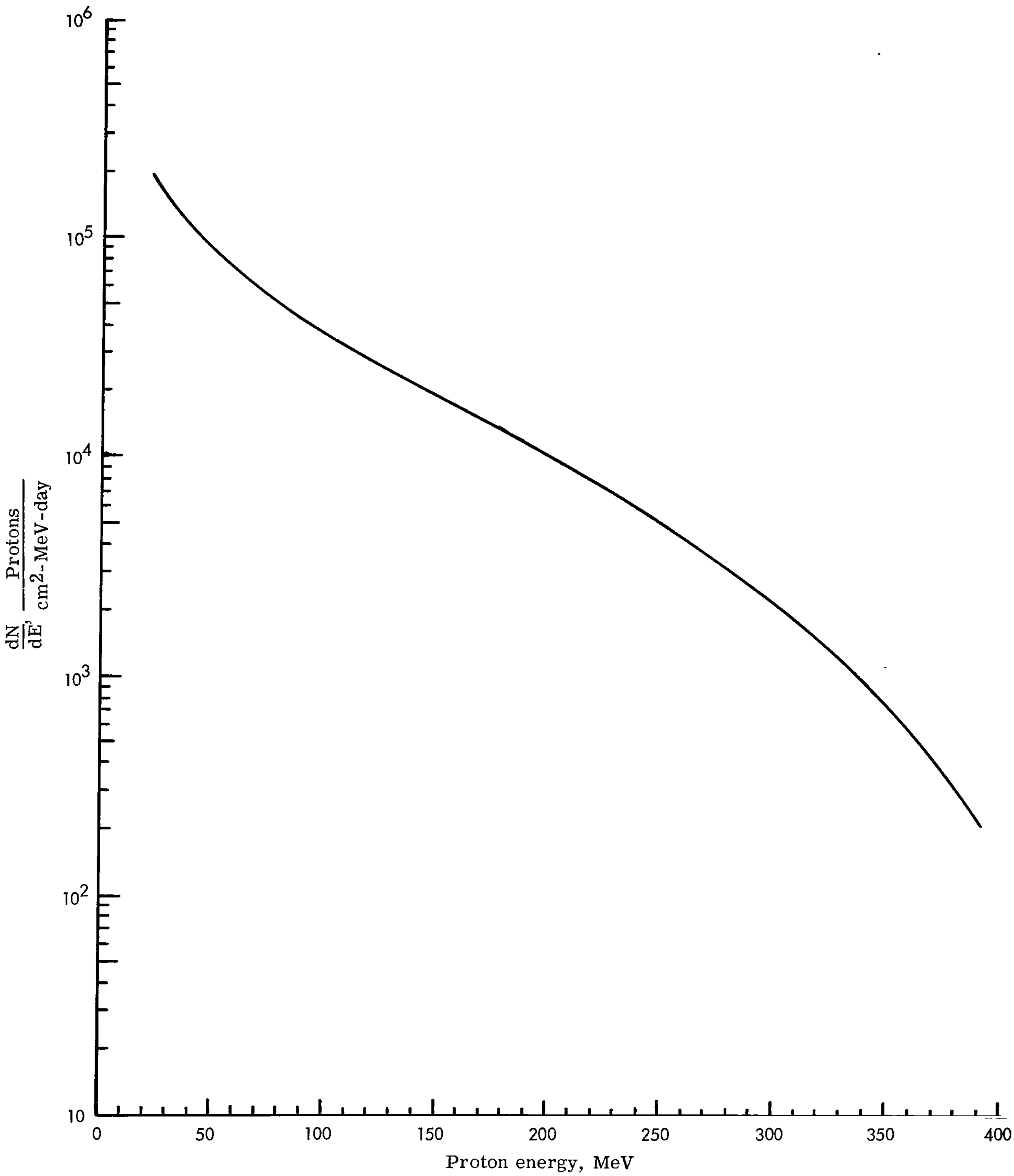

Figure 1.- Differential proton spectrum for an orbit of 350 nautical miles with 30° inclination and no shielding. Values were calculated by using the trajectory environment codes in reference 1.

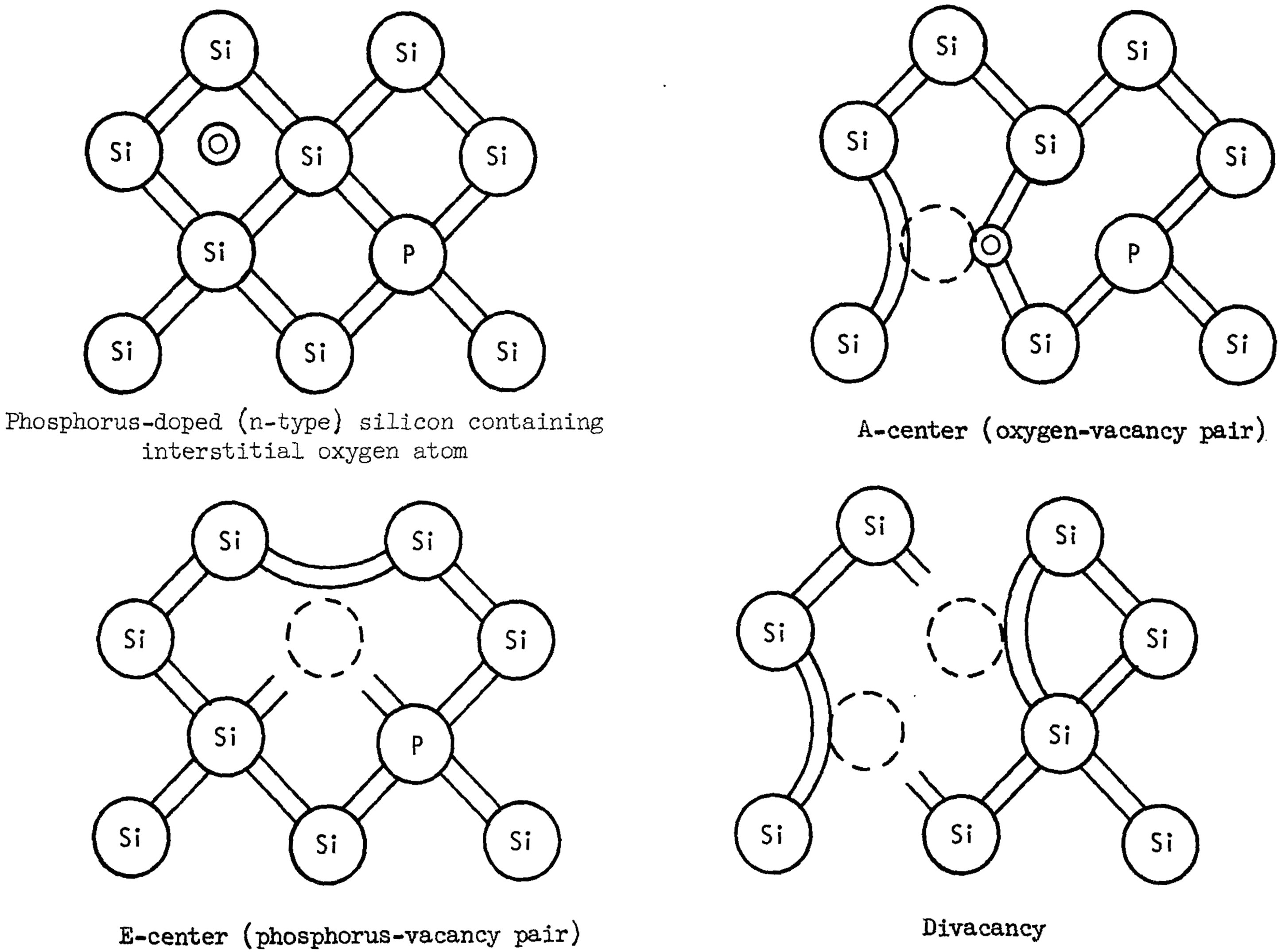

Figure 2.- Atomic model of phosphorus-doped (n-type) silicon and possible defect centers. Vacancies are represented by dashed circles.

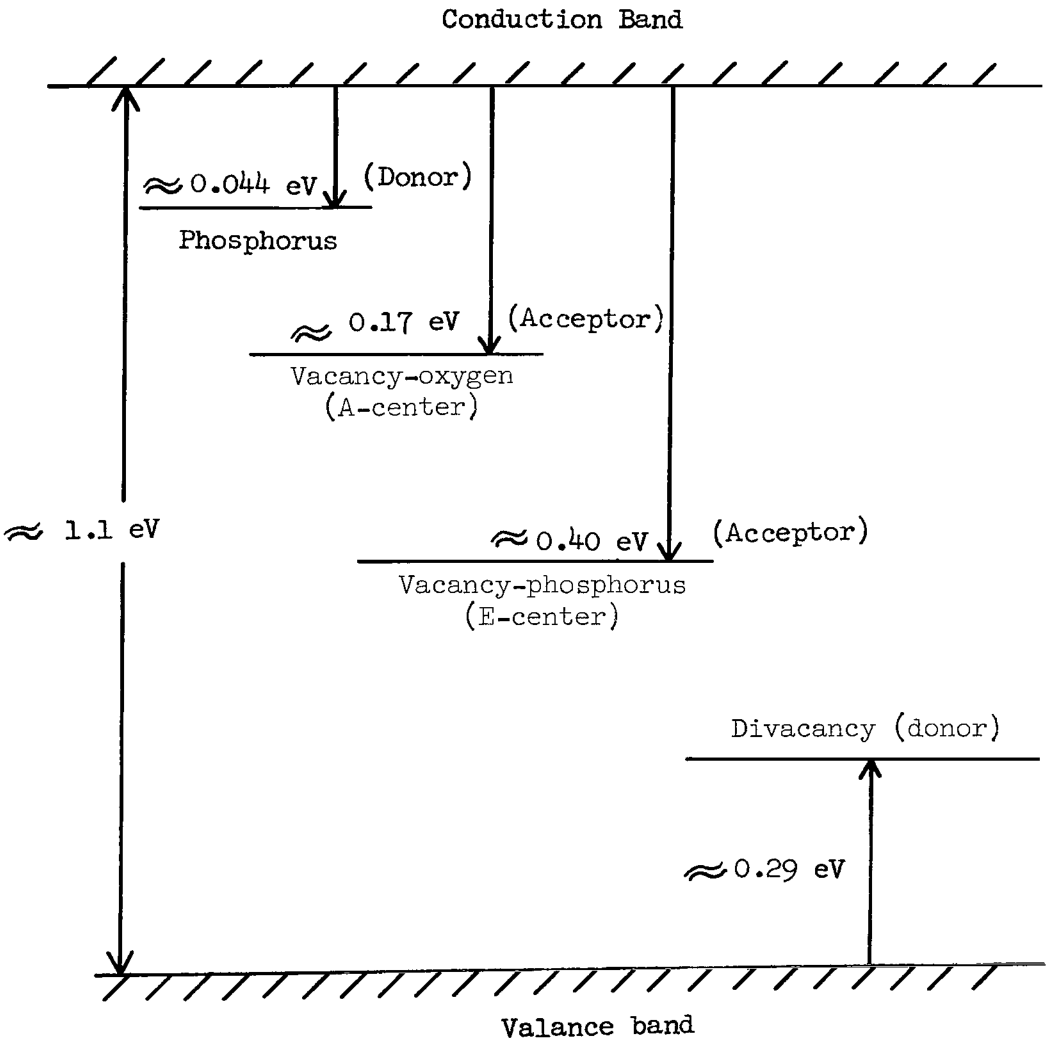

Figure 3.- Energy-level diagram for phosphorus-doped (n-type) silicon.

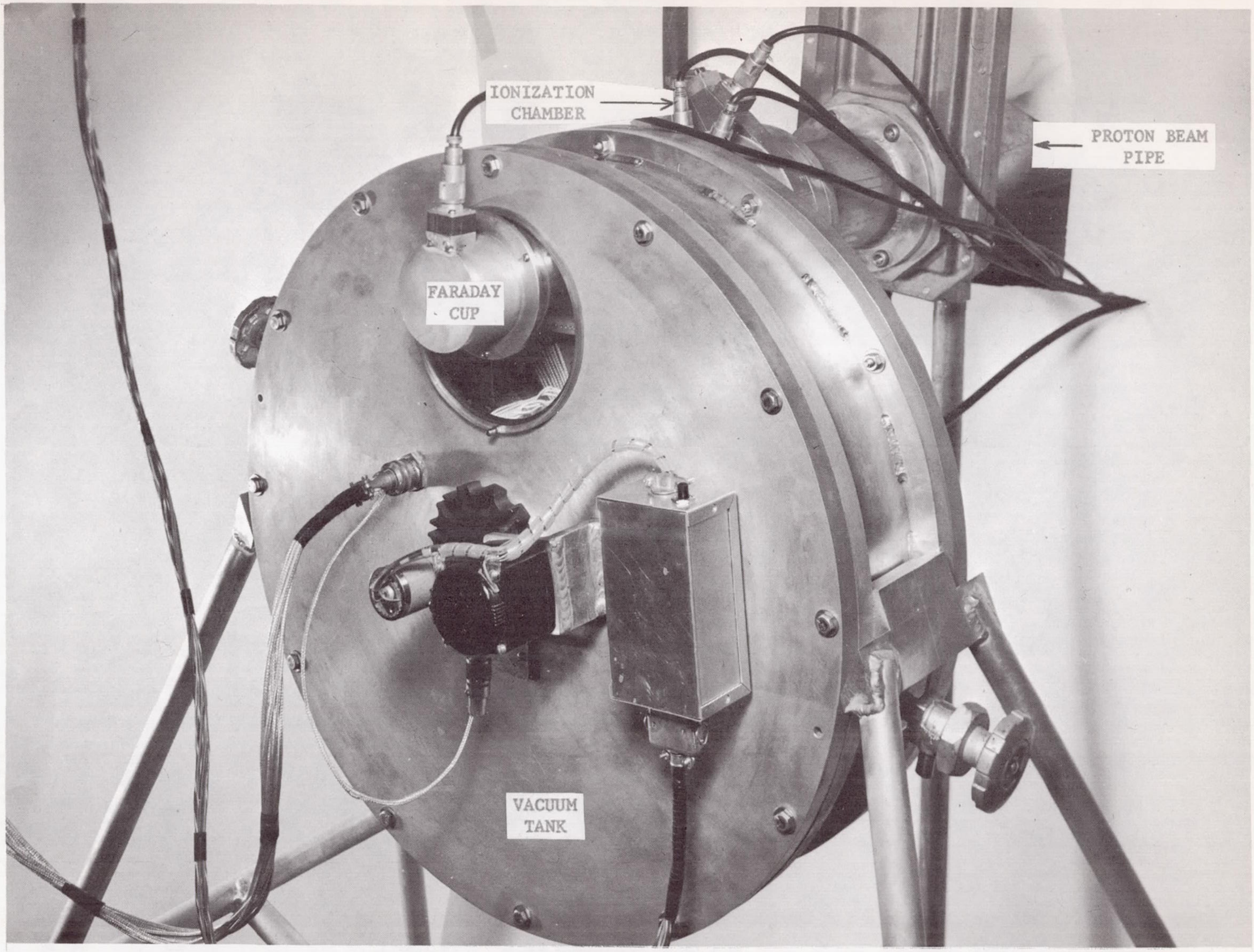

Figure 4.- Photograph of bombardment chamber used in the 22-MeV proton experiment.

L-69-1226

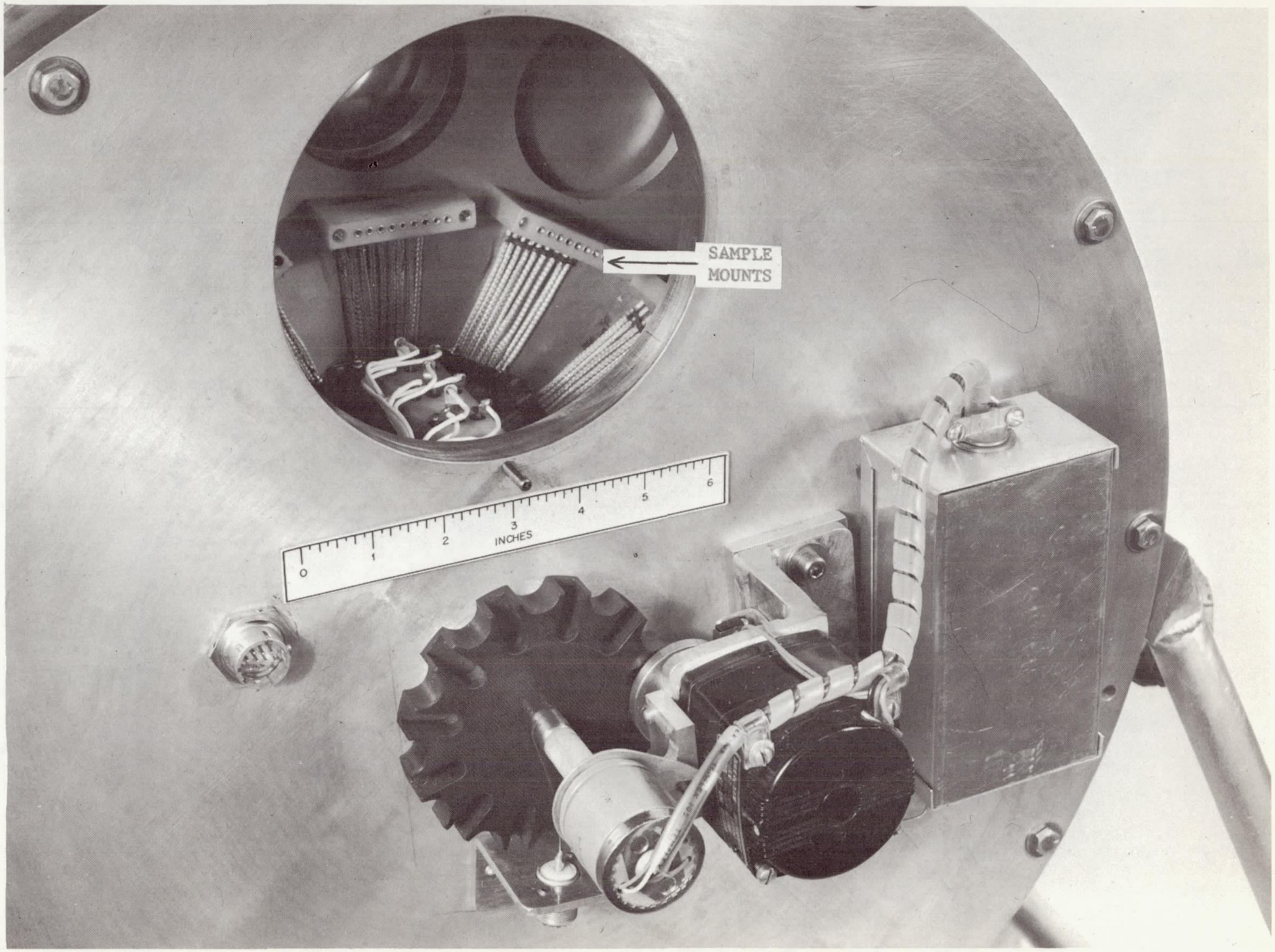

L-69-1227

Figure 5.- Photograph of bombardment chamber showing sample mounting.

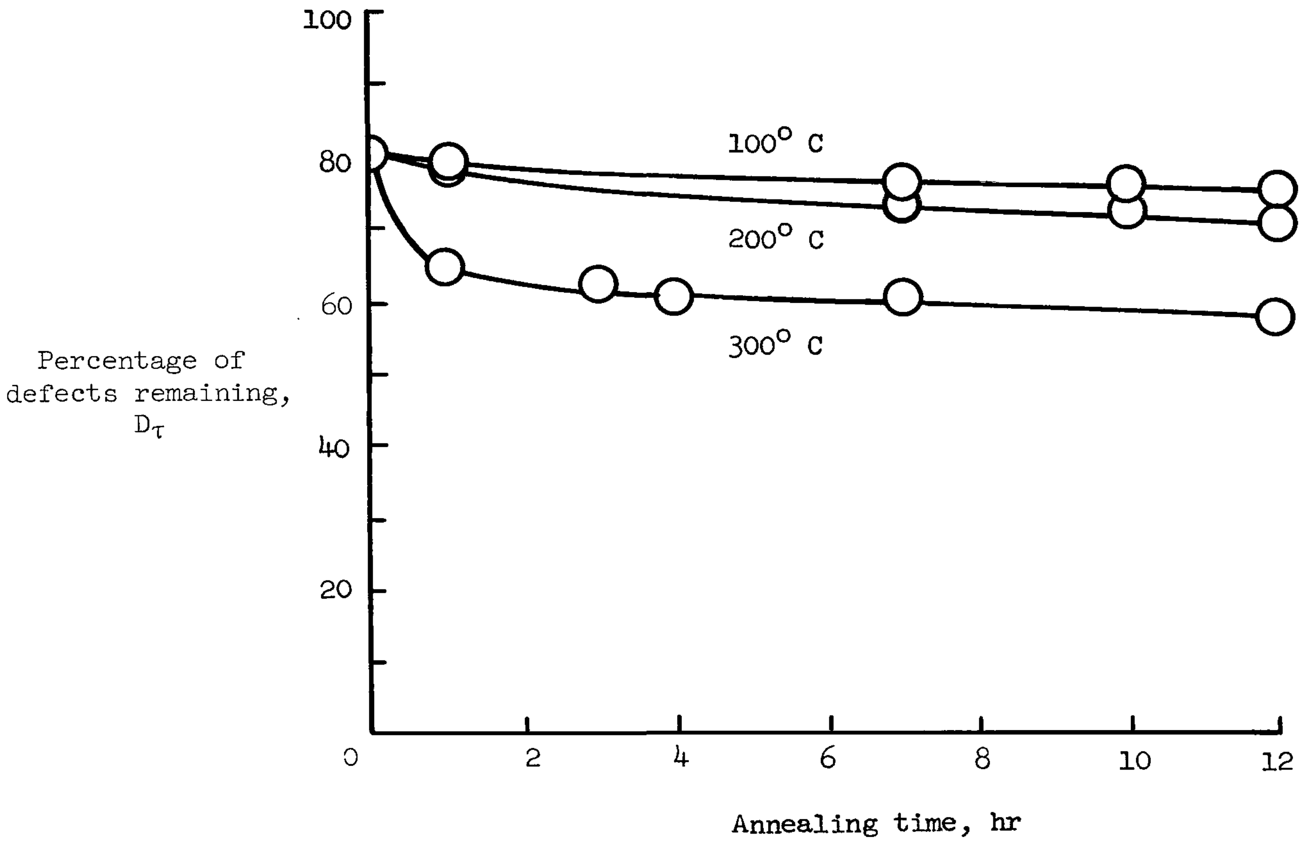

Figure 6.- Fraction of defects remaining in p-type silicon irradiated with 22-MeV protons to a fluence of $\Phi = 1 \times 10^{11}$ protons/cm^2 as a function of annealing time at 100° C, 200° C, and 300° C (unnormalized).

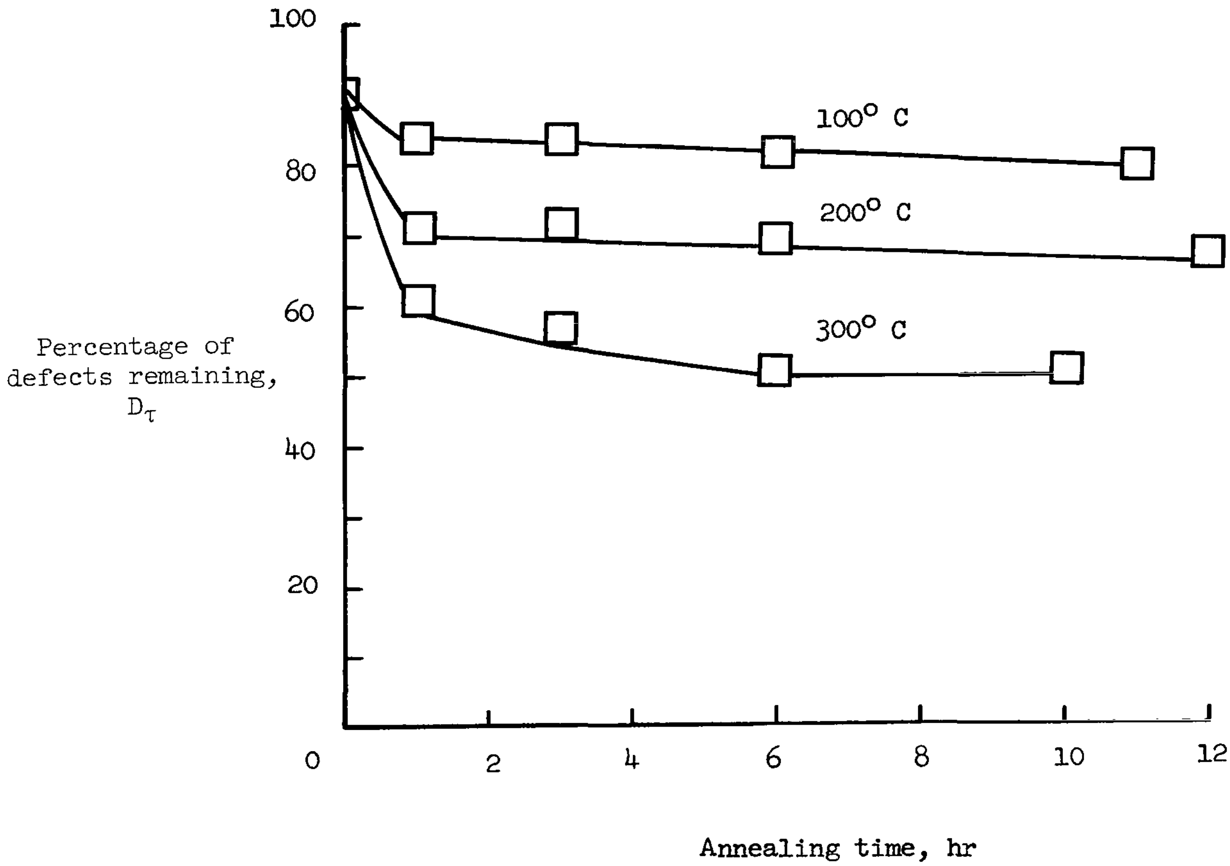

Figure 7.- Fraction of defects remaining in n-type silicon irradiated with 22-MeV protons to a fluence of $\Phi = 1 \times 10^{11}$ protons/cm^2 as a function of annealing time at 100° C, 200° C, and 300° C (unnormalized).

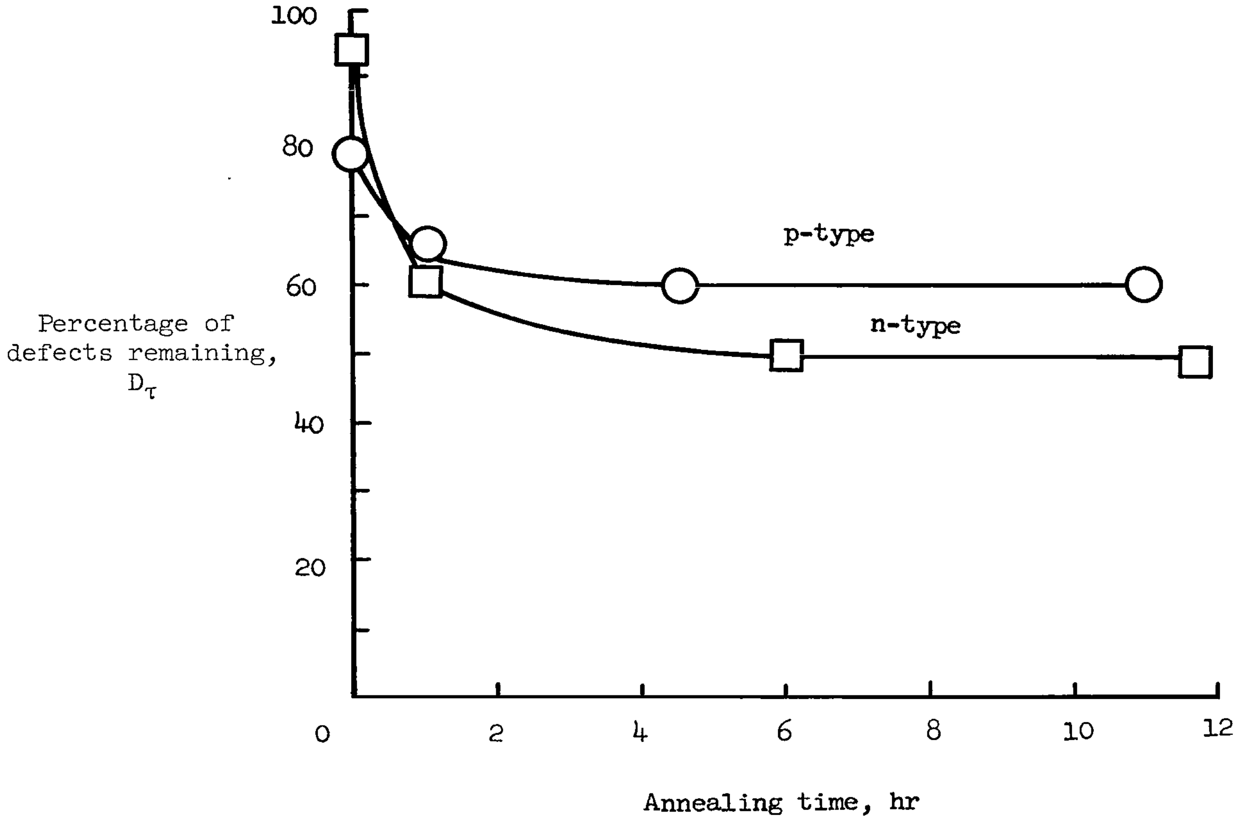

Figure 8.- Comparison of annealing of typical n- and p-type silicon samples at 300° C after irradiation with 22-MeV protons ($\Phi = 1 \times 10^{11}$ protons/cm^2) (unnormalized).

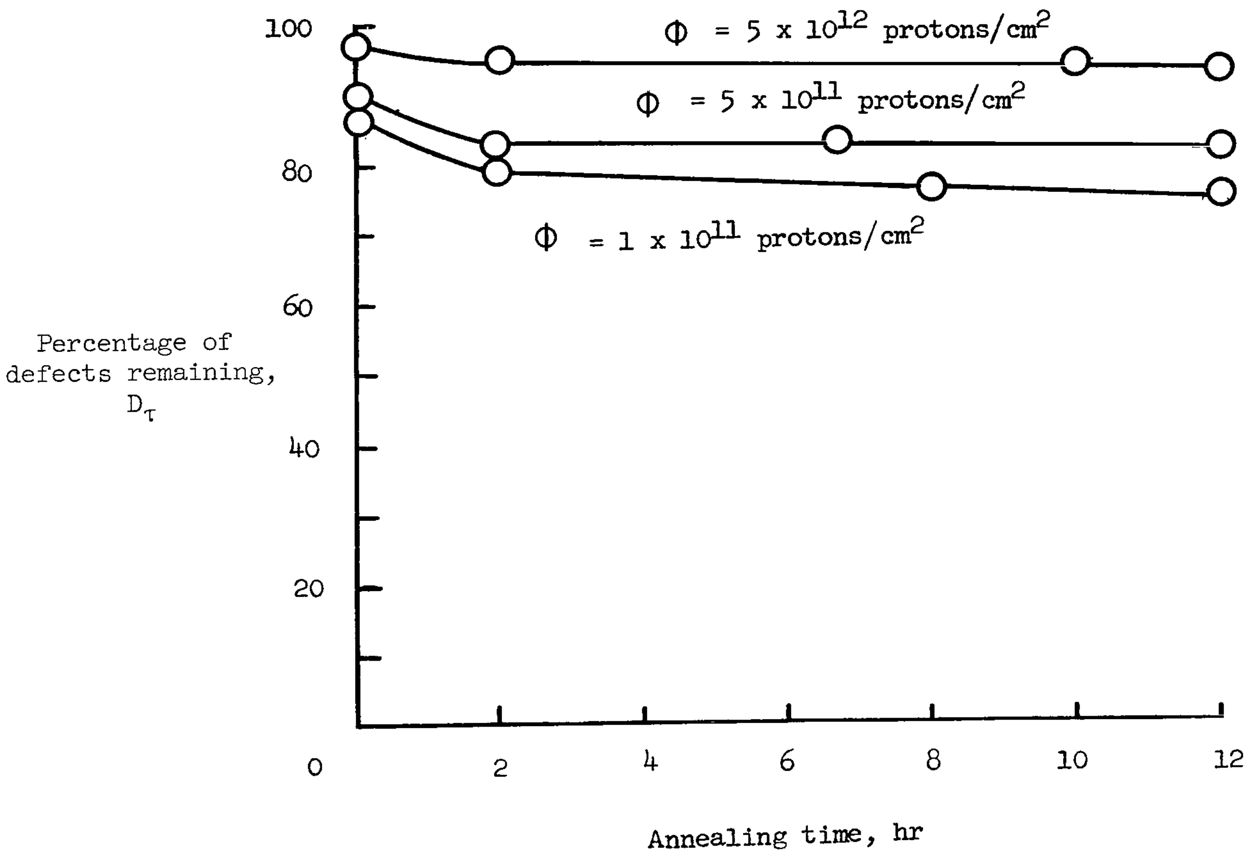

Figure 9.- Dependence of annealing of p-type silicon at 200° C on fluence of 22-MeV protons (unnormalized).

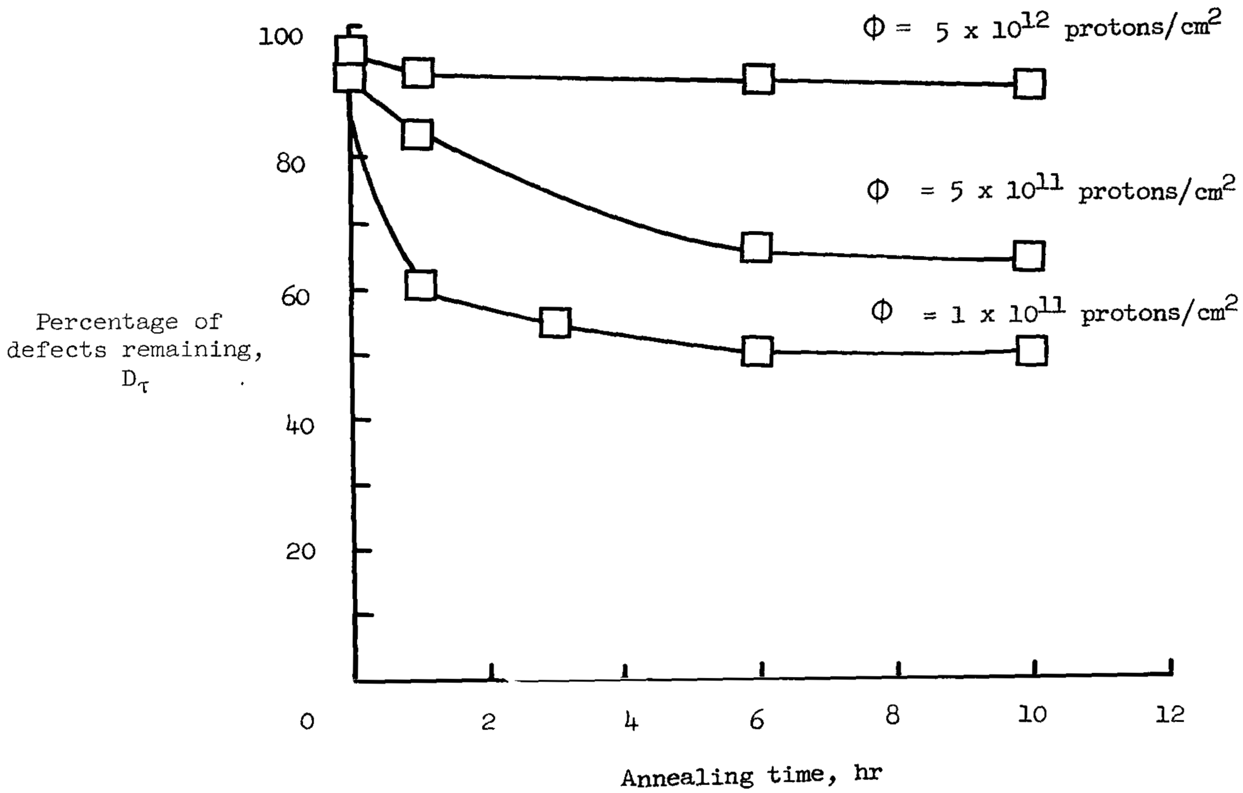

Figure 10.- Dependence of annealing of n-type silicon at 300° C on fluence of 22-MeV protons (unnormalized).

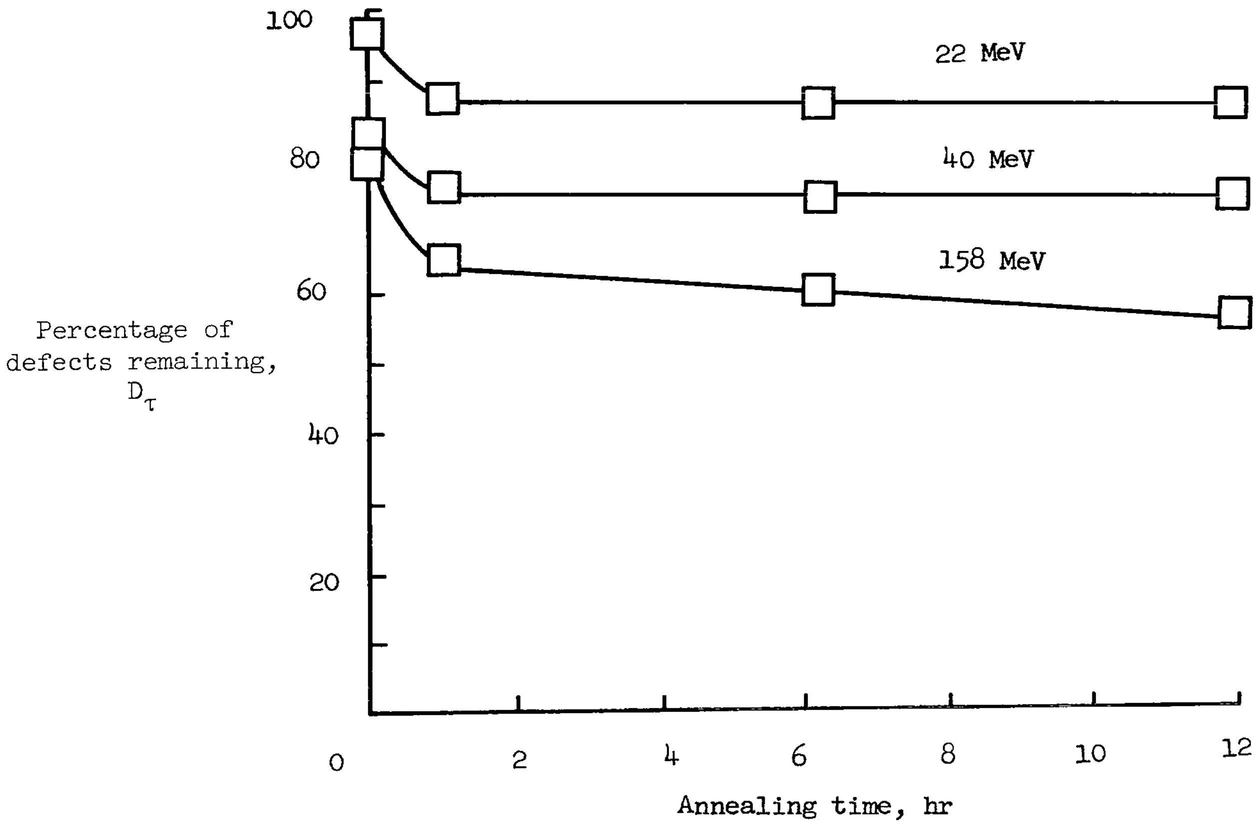

Figure 11.- Comparison of 22-, 40-, and 158-MeV proton annealing at 200° C for n-type silicon irradiated to a fluence of $\Phi = 1 \times 10^{12}$ protons/cm^2 (unnormalized).

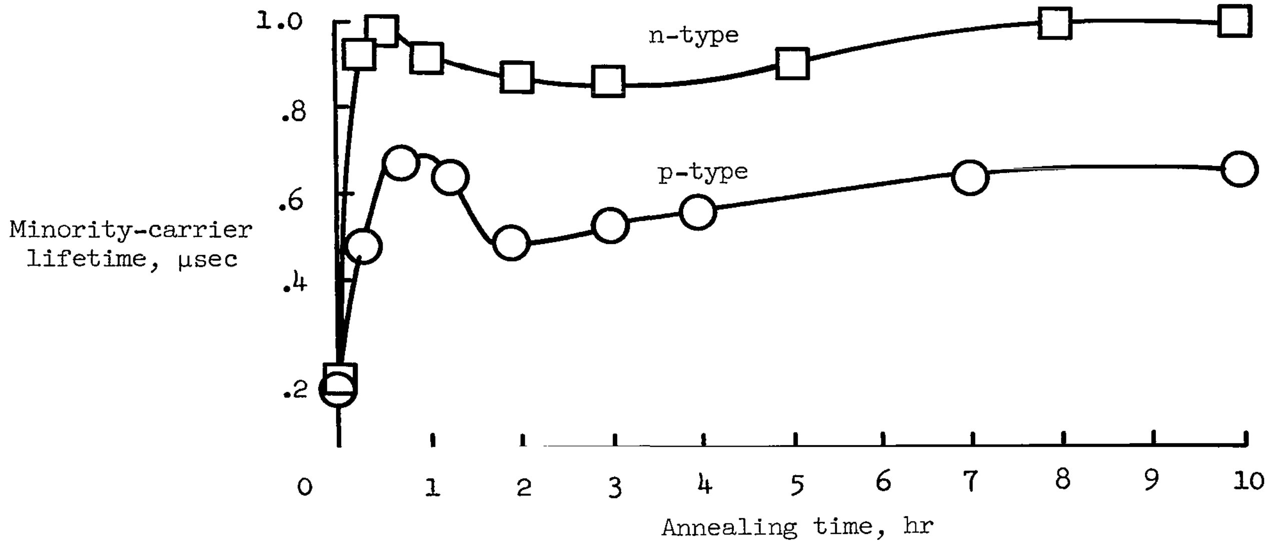

Figure 12.- Changes in minority-carrier lifetime (holes in n-type and electrons in p-type) for silicon irradiated with 22-MeV protons to a fluence of $\Phi = 1 \times 10^{12}$ protons/cm^2 and annealed at 300° C.

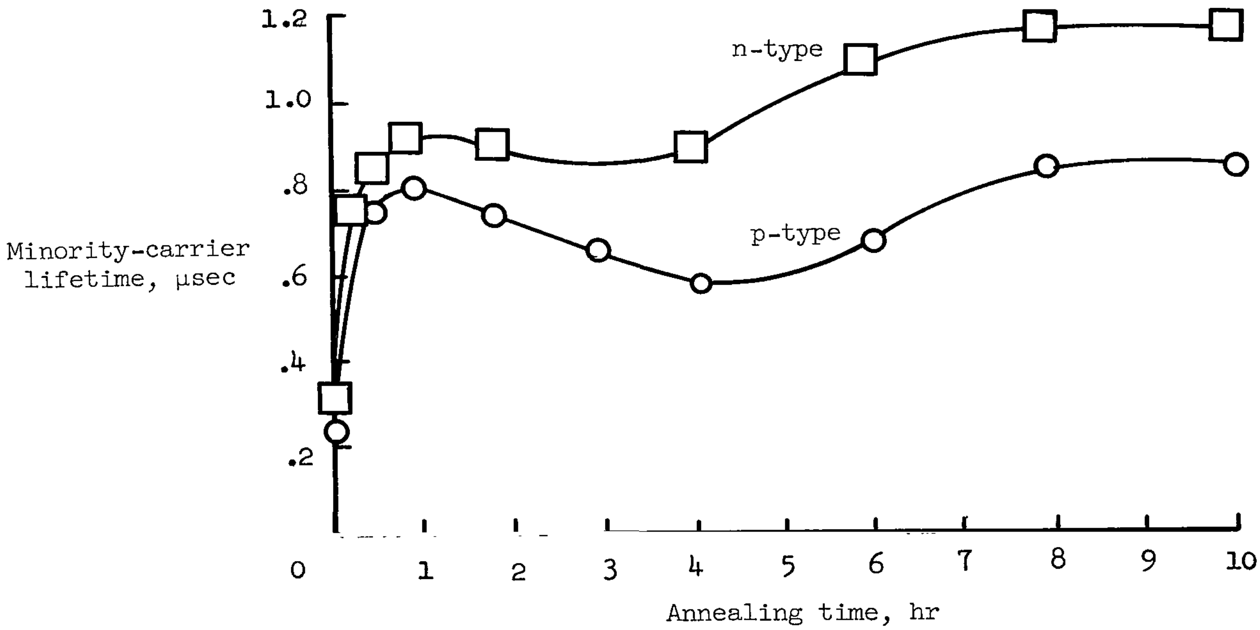

Figure 13.- Changes in minority-carrier lifetime (holes in n-type and electrons in p-type) for silicon irradiated with 22-MeV protons to a fluence of $\Phi = 1 \times 10^{10}$ protons/cm^2 and annealed at 300° C.

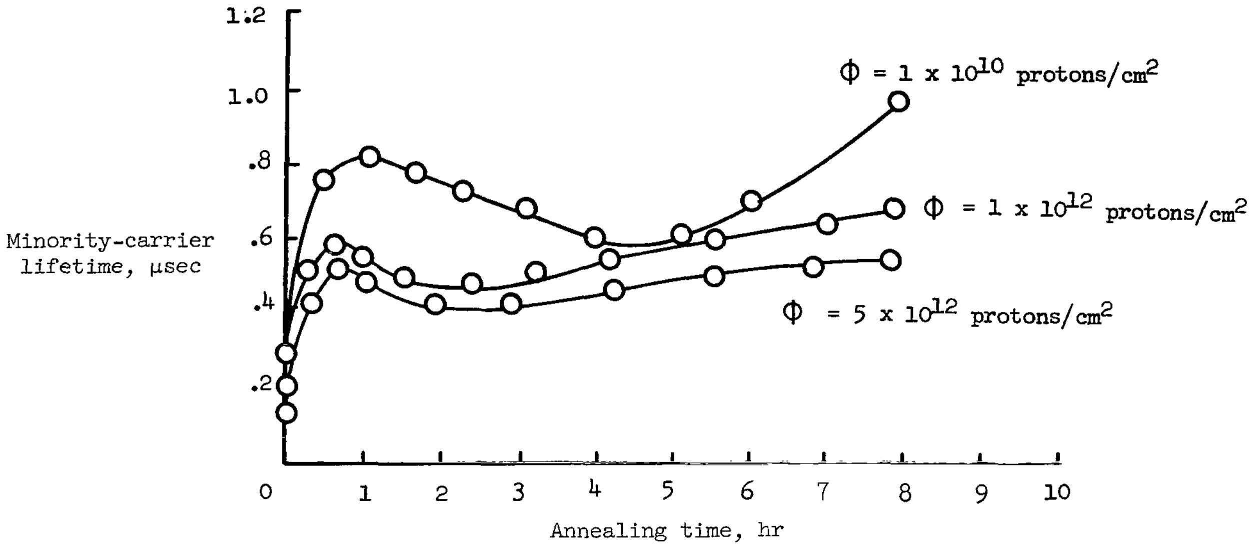

Figure 14.- Changes in minority-carrier lifetime (electrons) for p-type silicon irradiated to various 22-MeV proton fluences and annealed at 300° C.

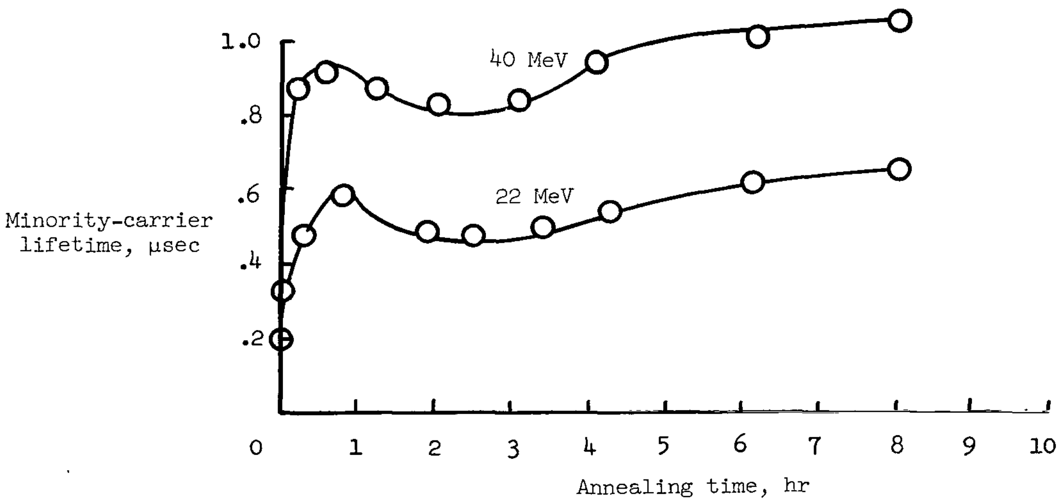

Figure 15.- Changes in minority-carrier lifetime (electrons) for p-type silicon irradiated with 22- and 40-MeV protons to a fluence of $\Phi = 1 \times 10^{12}$ protons/cm^2 and annealed at 300° C.

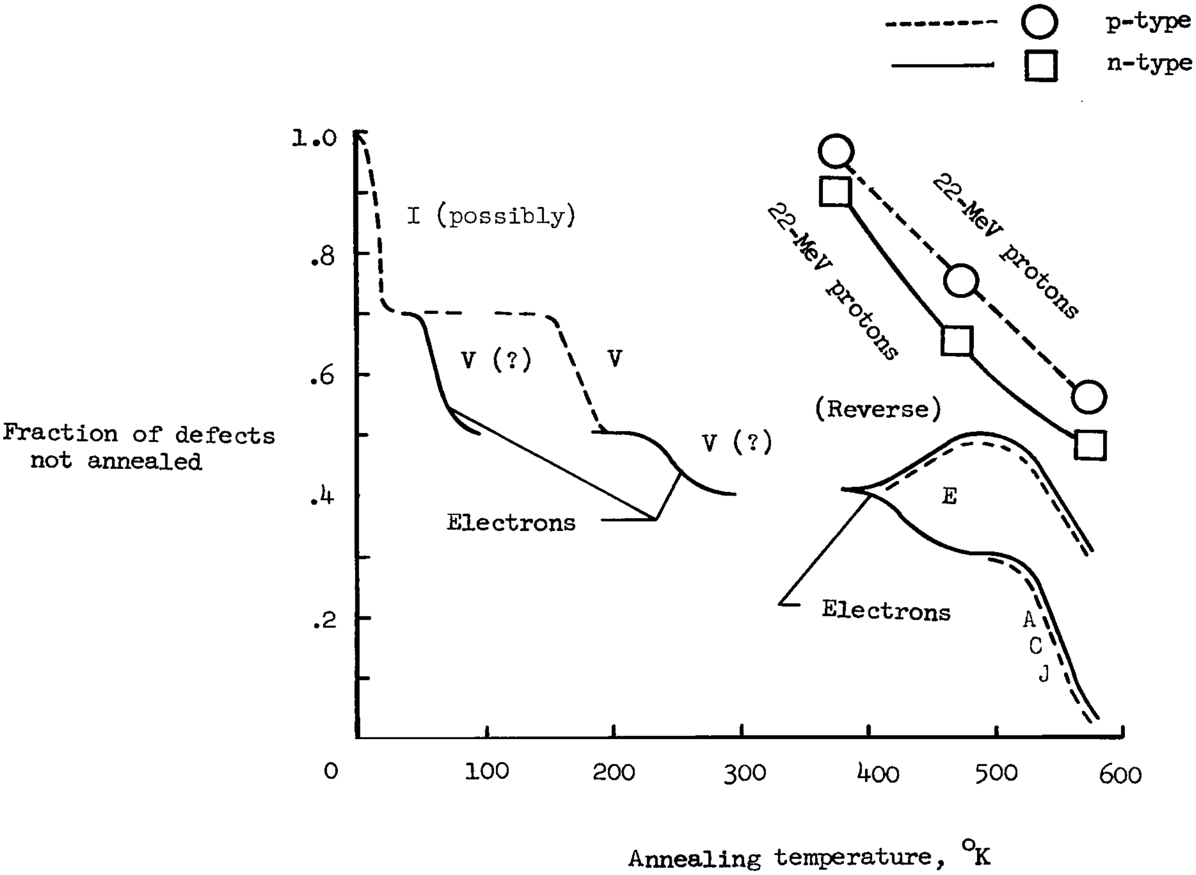

Figure 16.- Schematic diagrams of annealing stages in silicon.

"The aeronautical and space activities of the United States shall be conducted so as to contribute . . . to the expansion of human knowledge of phenomena in the atmosphere and space. The Administration shall provide for the widest practicable and appropriate dissemination of information concerning its activities and the results thereof."

—NATIONAL AERONAUTICS AND SPACE ACT OF 1958

NASA SCIENTIFIC AND TECHNICAL PUBLICATIONS

TECHNICAL REPORTS: Scientific and technical information considered important, complete, and a lasting contribution to existing knowledge.

TECHNICAL NOTES: Information less broad in scope but nevertheless of importance as a contribution to existing knowledge.

TECHNICAL MEMORANDUMS: Information receiving limited distribution because of preliminary data, security classification, or other reasons.

CONTRACTOR REPORTS: Scientific and technical information generated under a NASA contract or grant and considered an important contribution to existing knowledge.

TECHNICAL TRANSLATIONS: Information published in a foreign language considered to merit NASA distribution in English.

SPECIAL PUBLICATIONS: Information derived from or of value to NASA activities. Publications include conference proceedings, monographs, data compilations, handbooks, sourcebooks, and special bibliographies.

TECHNOLOGY UTILIZATION PUBLICATIONS: Information on technology used by NASA that may be of particular interest in commercial and other non-aerospace applications. Publications include Tech Briefs, Technology Utilization Reports and Notes, and Technology Surveys.

Details on the availability of these publications may be obtained from:

SCIENTIFIC AND TECHNICAL INFORMATION DIVISION

NATIONAL AERONAUTICS AND SPACE ADMINISTRATION

Washington, D.C. 20546